Journal of
METAMORPHIC GEOLOGY

J. metamorphic Geol., 2010, **28,** 753–768 doi:10.1111/j.1525-1314.2010.00889.x

Garnet–chloritoid–kyanite assemblages: eclogite facies indicators of subduction constraints in orogenic belts

A. J. SMYE, L. V. GREENWOOD* AND T. J. B. HOLLAND
Department of Earth Sciences, University of Cambridge, Cambridge CB2 3EQ, UK (as859@cam.ac.uk)

ABSTRACT The assemblage garnet–chloritoid–kyanite is shown to be quite common in high-pressure eclogite facies metapelites from orogenic belts around the world, and occurs over a narrowly restricted range of temperature ~550–600 °C, between 20 and 25 kbar. This assemblage is favoured particularly by large Al_2O_3:K_2O ratios allowing the development of kyanite in addition to garnet and chloritoid. Additionally, ferric iron and manganese also help stabilize chloritoid in this assemblage. Pseudosections for several bulk compositions illustrate these high-pressure assemblages, and a new thermodynamic model for white mica to include calcium and ferric iron was required to complete the calculations. It is extraordinary that so many orogenic eclogite facies rocks, both mafic eclogites *sensu stricto* as well as metapelites with the above assemblage, all yield temperatures within the range of 520–600 °C and peak pressures ~23 ± 3 kbar. Subduction of oceanic crust and its entrained associated sedimentary material must involve the top of the slab, where mafic and pelitic rocks may easily coexist, passing through these *P–T* conditions, such that rocks, if they proceed to further depths, are generally not returned to the surface. This, together with the tightly constrained range in peak temperatures which such eclogites experience, suggests thermal weakening being a major control on the depths at which crustal material is decoupled from the downgoing slab.

Key words: eclogite; garnet–chloritoid–kyanite; geodynamic modelling; pseudosection; thermal weakening.

INTRODUCTION

General background

High-pressure metamorphic rocks are a common feature of many Phanerozoic orogenic systems. Subduction of oceanic crustal material provides the best explanation for the genesis of *sensu stricto* eclogites and mafic blueschists. However, it has become increasingly apparent that the leading edges of continental domains and associated passive margins are also often subducted during convergent boundary activity (e.g. 1. Oman: Searle *et al.*, 1994; Warren *et al.*, 2003; Searle *et al.*, 2004; 2. Alps: Duchêne *et al.*, 1997; Kurz *et al.*, 1998, 1999; Rubatto & Hermann, 2001; 3. Himalaya: Sigoyer *et al.*, 2000; Leech *et al.*, 2005; Parrish *et al.*, 2006).

The advent of quantitative phase diagrams based on internally consistent thermodynamic data sets (e.g. Holland & Powell, 1990, 1998) has offered an insight into the pressure–temperature (*P–T*) evolution of subducted crust and, hence, a powerful constraint on the dynamics of convergent boundaries. Metamorphic modelling of mafic protoliths is hampered by the presence of high-variance mineral assemblages, the variable effect of oxidation state and ferric iron and the difficulty of constructing mixing models of complex mineral solid solutions (e.g. amphibole and clinopyroxene). In particular, typical high-pressure mafic assemblages are extremely susceptible to errors in reactive bulk composition and solution models. By contrast, accurate modelling of metamorphosed sediments can be undertaken in smaller chemical systems with fewer phases and with less complicated solid solutions. Thus, exhumed high-pressure metasedimentary rocks exposed in collisional orogenic settings yield an accessible means of tracking margin subduction. In this study the prime eclogite facies pelitic assemblage garnet–chloritoid–kyanite is examined via combined phase diagram modelling of typical pelitic bulk compositions and average *P–T* calculations using THERMOCALC version 3.33 (Holland & Powell, 1998). The results of these calculations are subsequently applied to the following questions regarding garnet–chloritoid–kyanite assemblages: (i) what controls the occurrence of this diagnostic high-*P* paragenesis? and (ii) what are the tectonic inferences to be deduced from its restricted *P–T* stability field? Samples of eclogite facies pelites from the Tauern window in the Eastern Alps and the Eastern Betic Cordillera of Spain are used in conjunction with published data to address these central aims.

**Present address*: Department of Earth and Environmental Sciences, The Open University, Walton Hall, Milton Keynes MK7 6AA, UK.

THE GARNET–CHLORITOID–KYANITE ASSEMBLAGE IN METAPELITES

Since the work of Harte (1975) and Harte & Hudson (1979) in preparing a semiquantitative petrogenetic grid for metapelites, and the first thermodynamic calibration of it in the KFMASH system by Powell & Holland (1990), it has been known that the assemblage garnet + chloritoid + kyanite in assemblages containing muscovite and quartz implies pressures greater than ~15 kbar at ~600 °C and is therefore probably restricted to eclogite facies conditions. Pelites containing this assemblage, such as TH-680 used below, were recognized (Holland, 1979) as belonging to the eclogite facies rocks of the Tauern Window, Austria, and as such assigned to conditions of ~20 kbar and 600 °C. Recently, understanding of phase relations in metapelites at elevated pressures has been greatly improved via experiments at high-pressure conditions (e.g. Schreyer, 1988; Massonne, 2000; Hermann, 2002). In addition, quantitative petrogenetic grids may now be constructed in model systems, such as KFMASH (Coggon & Holland, 2002; Wei & Powell, 2003) and NCKFMASH (Wei & Powell, 2006) which provide important insights into natural rock assemblages occurring in such high-*P* metamorphic domains. Such work confirms that the naturally occurring pelitic paragenesis, garnet–chloritoid–kyanite forms well within the eclogite facies.

Field occurrences

Despite previous studies claiming the rare nature of this assemblage (Gabriele *et al*., 2003; Negulescu *et al*., 2009), a survey of the relevant literature suggests that garnet–chloritoid–kyanite bearing schists are a common feature of tectonic environments in which subduction of pelitic material has occurred. The assemblage is reported from the following localities:

(i) *The Eastern Alps*. Eclogitic micaschists from the Eclogite Zone of the Tauern window (Miller, 1977; Holland, 1979; Miller *et al*., 1980; Stöckhert *et al*., 1997) contain chloritoid associated with garnet and kyanite. Thermobarometric studies (e.g. Holland, 1979; Spear & Franz, 1986) show that these metasedimentary rocks have experienced the same *P–T* evolution as hosted, mafic eclogite boudins, with peak conditions of ~20 kbar and 600 °C. Sample TH-680 investigated within this study comprises the following high-pressure assemblages: phengite, quartz, rutile, allanitic epidote, chloritoid, garnet and kyanite. The pervasive foliation, which wraps porphyroblastic phases, is defined by the shape-preferred orientation of phengite grains and quartz seams, and is locally, openly crenulated. Evidence for retrogressive mineral growth is confined to restricted patches of chlorite growth around the edges of chloritoid and garnet blasts. Garnet exists as rounded, millimetre-scale poikiloblasts which contain an inclusion assemblage dominated by phengite, quartz and rutile with subordinate amounts of chloritoid and kyanite. These inclusions commonly define sigmoidal fabric traces which are discordant to the matrix foliation. Chloritoid forms both millimetre-scale tablets within the matrix and also a ragged overgrowth around kyanite shards, suggesting two stages of growth. Kyanite exists in smaller quantities than both chloritoid and garnet as euhedral blasts within the matrix. Interestingly, margarite occurs as a rare, late-stage phase, overgrowing the penetrative phengite fabric.

(ii) *The Western Alps*. Vuichard & Ballevre (1988) reported the occurrence of garnet–chloritoid–kyanite and garnet–chloritoid–chlorite schists from within the high-pressure Sesia zone. The micaschists are located within the central portion of the zone, the Eclogitic Micaschist unit (Stella, 1894), and are associated with paragneisses, marbles and amphibolites. Collectively these rocks have experienced a complex polyphase tectonometamorphic evolution (Zucali *et al*., 2002), and peak metamorphic conditions were thought to have reached 17–21 kbar and 550–650 °C (Tropper *et al*., 1999) as a result of Paleogene subduction.

(iii) *The Carpathians*. Recent work by Negulescu *et al*. (2009) documents the presence of metasedimentary rocks containing garnet–chloritoid–kyanite bearing assemblages in association with retrogressed eclogites in the Bughea Complex of the Leaota Massif, South Carpathians. *P–T* calculations suggested that the assemblage formed at ~18 kbar and 580 °C prior to overprinting during exhumation.

(iv) *The Andes*. Gabriel *et al*. (2003) presented data from one of the few eclogite terranes within the Andean massif. The Raspas Complex of Ecuador, represents an exotic fragment of metamorphosed oceanic lithosphere, which comprises a suite of metaperidotites, eclogites and metapelites. Exhumation of the Raspas high-pressure rocks and the parent El Oro metamorphic complex resulted from and occurred during subduction and accretion of the Amotape–Chaucha terrane to pre-existing Mesozoic continental arc systems of the Eastern Cordillera (Feininger, 1980; Jaillard *et al*., 1990; Arculus *et al*., 1999). Raspas metasedimentary rocks contain the key garnet–chloritoid–kyanite assemblage along with the subset associations: garnet–chloritoid and garnet–chlorite. Peak metamorphic grade was estimated to be in the region of 20 kbar and 550–600 °C. The few existing geochronological constraints on the high-pressure evolution of these rocks suggest that they cooled through K–Ar closure during the late Cretaceous (Feininger & Silberman, 1982).

(v) *The Bohemian Massif*. Micaschists exposed in the central part of the Erzgebirge mountains, Saxothuringian domain of the Bohemian Massif (Czech Republic), display garnet–chloritoid–kyanite parageneses (Konopasek, 2001). The schists, which are intimately associated with mafic eclogites, were estimated to have equilibrated at conditions ~22 kbar and 640 °C.

(vi) *The Betics*. Garnet–chloritoid–kyanite–staurolite schist ALM-45 was collected by J. M. Baker as a loose block from the basement rocks of the Sierra Cabrera in south-eastern Spain, where the Carboneras fault zone outcrops at the coast near Macenas tower, between Mojaccar and Carboneras. This assemblage can also be observed in several other Betic localities (P. Agard pers. comm.). They comprise white, phengite-rich schists with apparently rotated garnet with strong C–S fabrics, presumably indicating extension during exhumation of these rocks from deep eclogite facies conditions. Fine-grained phengite and quartz-rich bands form a regionally pervasive foliation, which is crenulated at thin-section scale. Garnet commonly contains ring-shaped quartz inclusions, which are suggestive of an intermittent growth history. The unusual presence of some staurolite, which is often present in the form of corroded relic grains in close association with quartz and phengite, is enigmatic, as calculations (see later) suggest that the pressures were too high for this phase. It may be that staurolite persisted during compression into the eclogite facies, or, alternatively that the staurolite grew later during decompression. Some kyanite is partially overgrown by staurolite, whereas some staurolite entrap a folded fabric, making textures ambiguous. Kyanite itself forms millimetre-scale porphyroblasts within the matrix and, as with chloritoid blasts, is often overgrown by a fine-grained phengite fabric. Porphyroblastic tablets of chloritoid are common within the matrix indicating its growth early within the rock's history. Analyses of the principal minerals are provided in the Appendix.

(vii) *The Kokchetav Block*. Udovkina *et al*. (1977) and Massonne & Schreyer (1989) described metapelites from the Kokchetav Block of northern Kazakhstan as containing garnet poikiloblasts enclosing chlorite and chloritoid inclusions within a matrix of talc and kyanite.

(viii) *The Norwegian Caledonides*. Chauvet *et al*. (1992) and Hacker *et al*. (2003) reported subassemblages of garnet–chloritoid–kyanite–staurolite–paragonite–muscovite–quartz within highly aluminous pelitic horizons of the Gåsetjœrn unit, which are interleaved with the Western Gneiss Complex. Here, staurolite is thought to be a member of the peak assemblage, which is reflected in peak *P–T* estimates of 14–16 kbar at 575–600 °C (Hacker *et al*., 2003) – slightly lower in pressure than the staurolite-absent garnet–chloritoid–kyanite assemblages reported above. For this reason, these rocks fall outside of the paper's remit.

Thus, it appears that the diagnostic garnet + chloritoid + kyanite assemblage is relatively widespread in its occurrence worldwide, and provides a useful indicator of eclogite facies conditions from pelitic rocks, even if mafic rocks are not present.

CONSTRAINING THE *P–T* CONDITIONS OF FORMATION

Construction of pseudosections and petrogenetic grids for high-*P* pelites within KFMASH yield important information on expected phase relations at eclogitic conditions. Coggon & Holland (2002) took an average Dalradian pelite composition and constructed a *P–T* pseudosection involving garnet, kyanite/sillimanite, carpholite, chloritoid, biotite, chlorite, staurolite, quartz/coesite and H_2O between 5 and 27 kbar and 300 and 750 °C. The calculated equilibria show that the garnet–chloritoid–kyanite paragenesis is stable over a surprisingly limited region of *P–T* space, approximately between 23 and 25 kbar and 590 and 600 °C. Given the number of localities from which garnet–chloritoid–kyanite-bearing metasedimentary rocks have been reported, it is of major importance to investigate the bulk compositional controls on this eclogite facies paragenesis.

Pseudosection modelling

This contribution presents a series of *P–T* pseudosections, starting with the basic KFMASH system and progressively incorporating Na_2O, CaO, Fe_2O_3 and MnO to form the extended pelitic model system, MnNCKFMASHO, for a garnet–chloritoid–kyanite schist (sample TH-680) from the Eclogite zone, Tauern window, south-central Austria. This is done incrementally to examine the bulk compositional controls on garnet–chloritoid–kyanite assemblages. Pseudosection calculations were carried out using THERMOCALC v. 3.33 software. Bulk compositions for the target sample TH-680 were calculated by combining mineral modes and electron microprobe mineral analyses. In accordance with phases present in TH-680, equilibria have been calculated for the *P–T* window, 14–30 kbar and 500–625 °C involving garnet, kyanite, chloritoid, carpholite, chlorite, epidote, paragonite, jadeite with quartz/coesite, muscovite and H_2O taken to be in excess (see Discussion). TiO_2 is ignored in all calculated diagrams because rutile is the only Ti-bearing phase present in these rocks and all other phases have extremely low Ti contents.

White mica mixing models

In order to model the white mica in systems with calcium and ferric iron, the mixing parameters for margarite (ma) and ferrimuscovite (fmu) end-members need to be added to the simpler white mica model of Coggon & Holland (2002). The brittle mica margarite also requires consideration as a separate phase because it occurs in rock TH-680 as late cross-cutting laths grown during subsequent decompression and later Alpine metamorphism.

The following discussion illustrates the addition of margarite as a phase and incorporation of the ma end-member into muscovite and paragonite. Details of addition of the fmu end-member follow afterwards. Coggon & Holland (2002) built a white mica model for phengite and paragonite in the simple KNCFMASH system, and included the end-members muscovite

(mu), paragonite (pa), celadonite (cel) and ferroceladonite (fcel) to describe white mica related by the muscovite–paragonite solvus. Introduction of the ma end-member [$CaAl_2(Al_2Si_2)O_{10}OH_2$] into the model is not straightforward in the absence of any reliable experimental data on paragonite–margarite mixing. Early work by Hinrichsen & Schurmann (1971) found only single-phase mica across the join, but later work by Franz *et al.* (1977) concluded that a very asymmetric miscibility gap exists which closes just above 600 °C. However, the experimentally determined gap is much too narrow in composition to match the natural examples of coexisting paragonite–margarite pairs (e.g. Ackermand & Morteani, 1973; Höck, 1974; Bucher-Nurminen *et al.*, 1983; Feenstra, 1996). We have therefore elected to use these natural coexisting mica in the modelling, in particular by fitting the mixing parameters involving margarite to coexisting triplets of muscovite + margarite + paragonite. Although the available data are sparse, and estimates of the prevailing pressures and temperatures are only known approximately, useful preliminary data may be obtained.

Eliminating several coexisting mica triplets on the basis of retrograde reaction involving replacement of aluminosilicate by ma + pa + mu (Guidotti & Cheney, 1976; Guidotti *et al.*, 1979; Baltatzis & Katagas, 1981), it was decided to use the data of Höck (1974); Okuyama-Kusunose (1985) and Feenstra (1996). All these rocks come from the greenschist to amphibolite transition, assumed to have been metamorphosed at ~6–7 kbar and 450–550 °C. All the data are plotted in Fig. 1 where the compositions of coexisting triplets are quite similar and therefore formed over a small range of conditions. The data of Feenstra (1996) from Naxos come from rocks of zone III just below the staurolite isograd, and probably represent temperatures ~550 °C.

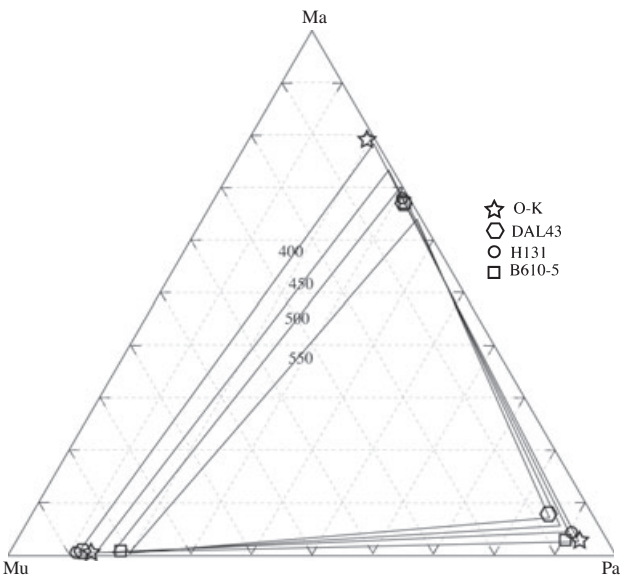

Fig. 1. Muscovite–paragonite–margarite compositions from the literature. Symbols: star, 400–450 °C, Okuyama-Kusunose (1985); circle, 450–500 °C, Höck (1974); square, 500 °C, Feenstra (1996); hexagon, 550 °C, Feenstra (1996). Lines contoured for temperature using the parameters from this study at 6-kbar pressure.

The parameters used by Coggon & Holland (2002) will be taken to apply, except that the $W_{cel\ pa}$ interaction energy is now assumed to be pressure dependent such that appropriately smaller values are used for low pressures (see comments of Keller *et al.*, 2005). Any observed asymmetry will be taken into account by use of the van Laar model as formulated by Holland & Powell (2003). Here, we make the simplest assumption that the ma and fmu end-members have the same asymmetry parameters as muscovite.

The site partitioning scheme of the white mica model for all three phases (mu, pa and ma) is assumed as follows:

	A	M2A	M2B	T1	T2
mu	K	Al	Al	SiAl	Si_2
cel	K	Mg	Al	Si_2	Si_2
fcel	K	Fe	Al	Si_2	Si_2
pa	Na	Al	Al	SiAl	Si_2
ma	Ca	Al	Al	Al_2	Si_2
fmu	K	Al	Fe^{3+}	SiAl	Si_2

The basic model of Coggon & Holland (2002) provides the interaction energies among the first four end-members above, and those involving ma and fmu need to be determined. As margarite is a brittle mica with a structure different to that of muscovite and paragonite, there will additionally be free energy increments to the ma end-member in both muscovite and paragonite as well as free energy increments to the mu, cel, fcel, pa and fmu end-members in the margarite phase reflecting this structural difference.

As there are so few data available, and as the regions of composition occupied by the mica is so restricted by the wide solvi and miscibility gaps (Fig. 1), we may reasonably take the basic interactions found for muscovite and paragonite and apply them to the margarite phase. The widths of the solvi depend critically on the parameters $W_{mu.pa}$, $W_{mu.ma}$ and $W_{ma.pa}$, while the positions of the apices of the three-phase field are extremely sensitive to the exact values of the DQF parameters (Gibbs energy increments in the sense of Powell, 1987) both for pa in margarite and for ma in muscovite and paragonite. To get an agreement with Fig. 1 at pressures of 6 kbar and temperatures of 450–550 °C, particularly to keep the Ca content of muscovite and the K content of margarite very low, it required a large value for $W_{mu.ma}$=35 kJ. As margarite takes in very little celadonite, the value of $W_{cel.ma}$ was set a little higher at 40 kJ. Likewise, because of the similarity in size and charge between Fe and Mg, $W_{fcel.ma}$ was also set at 40 kJ. Part of the asymmetry in

the margarite–paragonite gap is explained by the van Laar volume parameters (α_{pa}=0.37, α_{ma}=0.63), but it was necessary to make $W_{pa.ma}$ equal to 15 kJ in the muscovite and paragonite phases but only 13 kJ in the margarite phase. These values ensured that the width in the miscibility gaps matched those seen in (Fig. 1). In addition, a small Gibbs free energy increment of 3.0 kJ needed to be added onto the ma end-member in paragonite and muscovite. Likewise 1.0 kJ was added onto mu cel and fcel end-members and 1.2 kJ onto the pa end-member in margarite.

Addition of the fmu end-member can be done more simply as there are virtually no data at hand, and the simplest model is used which will allow incorporation of a small ferric iron content into the M2B site. Thus, the fmu end-member is taken as mixing ideally with all other end-members, and any non-ideality present is assumed to be absorbed into the Gibbs free energy, which was adjusted to produce ferric iron contents in mica similar to those coexisting with ilmenite and magnetite (Dyar *et al*., 2002). The final model parameters for muscovite and paragonite and for margarite are given in the Appendix. In all the calculations with the program THERMOCALC for fitting to Fig. 1, the phengite was constrained to have silica contents of 3.15 c.p.f.u, based on Coggon & Holland (2002) and an assumed very low ferric content. The Fe/(Fe + Mg) content of phengite in Fig. 1 is immaterial as the interactions involving Fe are assumed equal to those involving Mg but was fixed at 0.5 in the calculations.

Given the scatter in analyses and uncertainties in assigned pressures and temperatures, Fig. 1 shows that the thermodynamic model parameters provide reasonable agreement with the natural mineral compositions. With this new mica model, pseudosection calculations may be done in systems larger than the simple KFMASH diagram of Coggon & Holland (2002). Below we present a series of diagrams, using the TH-680 bulk composition, in the KFMASH, NCKFMASH, NCKFMASHO and MnNCKFMASO systems to investigate the position and size of the garnet + chloritoid + kyanite field in *P–T* space. All pseudosections are contoured for X_{Fe}^{gt} and Si content in phengite.

(i) *The KFMASH subsystem*. The simple KFMASH pseudosection (Fig. 2) is characterized by the prevalence of trivariant and divariant fields, with only two quadrivariant fields seen by the specified bulk composition. The garnet–chloritoid–kyanite stability field occupies a thin sliver of *P–T* space in the region, 18–27 kbar and 540–610 °C. The lower and upper temperatures of the assemblage is defined by the kyanite-in and chloritoid-out boundaries respectively. In turn, upper and lower pressure maxima are delineated by univariant reactions involving the growth of carpholite and chlorite, both at the expense of chloritoid. Of particular interest is the expansive, trivariant

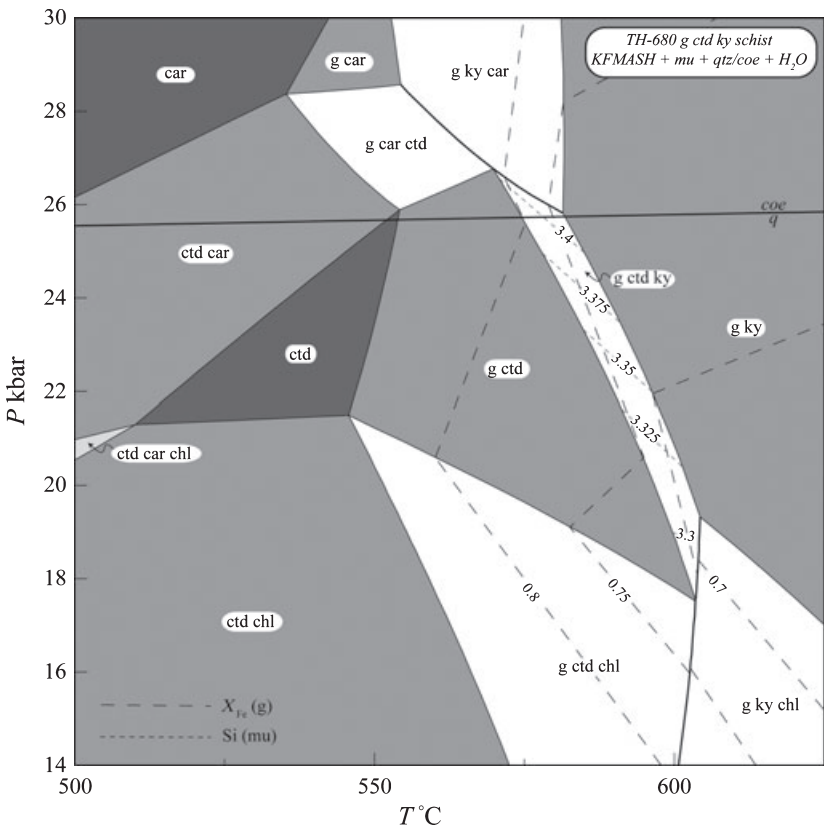

Fig. 2. KFMASH pseudosection for rock TH-680. Bulk composition used: SiO_2, 72.93; Al_2O_3, 14.28; MgO, 3.77; FeO, 5.36; K_2O, 3.66.

garnet–kyanite field at higher temperatures than the garnet–chloritoid–kyanite assemblage. This trivariant (in KFMASH) assemblage, garnet–kyanite–phengite–quartz, is observed in metapelites of the central Alpine, Adula nappe (Meyre *et al.*, 1999; Dale & Holland, 2003). The bulk composition TH-680 is characterized by a considerably larger *P–T* field for the gt–ky–ctd assemblage than seen in the average Dalradian pelite of Coggon & Holland (2002).

(ii) *The NCKFMASH subsystem*. The incorporation of Na_2O and CaO into the model system introduces the new phases, jadeite and paragonite into pseudosection calculations, as well as the use of extended activity–composition models for sodium- and calcium-bearing phases. The pseudosection (Fig. 3) differs from that calculated within KFMASH in that it is dominated by quadrivariant fields. The foundations of the KFMASH topology remain, with a strongly temperature sensitive garnet–chloritoid–kyanite field situated down temperature of the large garnet–kyanite domain. However, it can be seen that univariant reactions involving the growth of chlorite and carpholite at the expense of chloritoid, enlarge to form trivariant fields. Paragonite only occurs at low temperatures between 20 and 23 kbar. The garnet–chloritoid–kyanite association covers a wider temperature range but smaller pressure range as a result of the larger chemical system but still remains a relatively small stability field in the region of 19–24.5 kbar and 560–590 °C. Jadeite is restricted to the highest pressures but occurs in such low modal amounts that it would probably be undetectable in thin section even if it were to survive decompression.

(iii) *The NCKFMASHO subsystem*. Rock TH-680 contains only a small amount of ferric iron, as reflected in a few epidote grains visible in thin section. Expanding the chemical system to include ferric iron and the extra phase epidote in calculations requires the use of extended activity models for mica, garnet, chloritoid, chlorite and jadeite. Major differences to the NCKFMASH topology (Fig. 4) comprise the appearance of a low-*T* garnet stability boundary, the presence of epidote in all fields, except at the highest pressures and temperatures, and further extension of the important garnet–chloritoid–kyanite (±epidote) field to slightly lower pressures. The epidote occurs in small amounts, less than 2% modally, in agreement with the petrographic observations. Ferric iron in the bulk composition reduces paragonite stability to lower temperatures than shown on the diagram.

(iv) *The MnNCKFMASHO system*. The pseudosection (Fig. 5) was constructed because it is well known that manganese fractionates particularly strongly into garnet, chloritoid and carpholite, stabilizing these phases in rocks. The amount of manganese added takes into account the fact that garnet growth initiated well before attaining peak conditions of interest. Therefore, garnet rim chemistry provides a more realistic estimate of the reactive bulk composition than core regions.

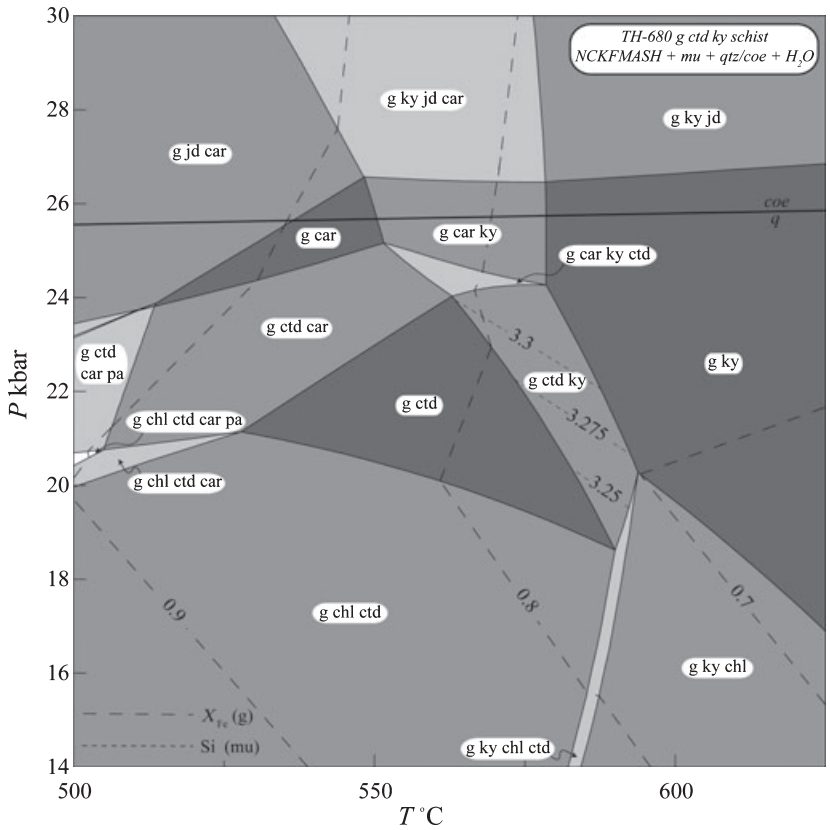

Fig. 3. NCKFMASH pseudosection for rock TH-680. Bulk composition used: SiO_2, 71.80; Al_2O_3, 14.06; CaO, 1.32; MgO, 3.71; FeO, 5.27; K_2O, 3.60; Na_2O, 0.24.

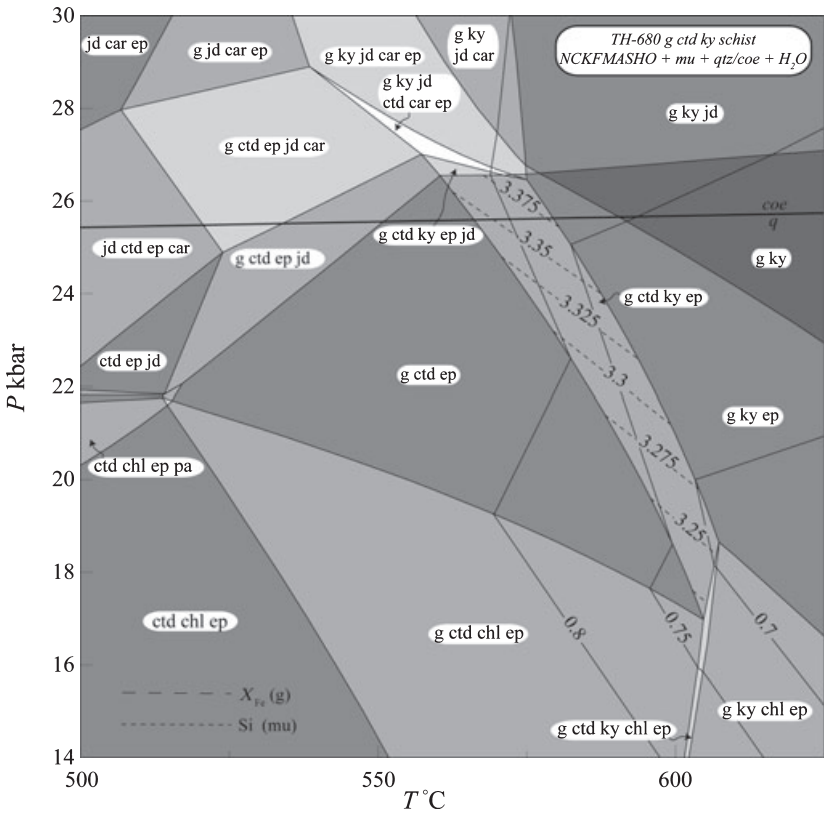

Fig. 4. NCKFMASHO pseudosection for rock TH-680. Bulk composition used: SiO_2, 70.31; Al_2O_3, 13.76; CaO, 1.29; MgO, 3.64; FeO, 6.53; K_2O, 3.53; Na_2O, 0.24; O, 0.70.

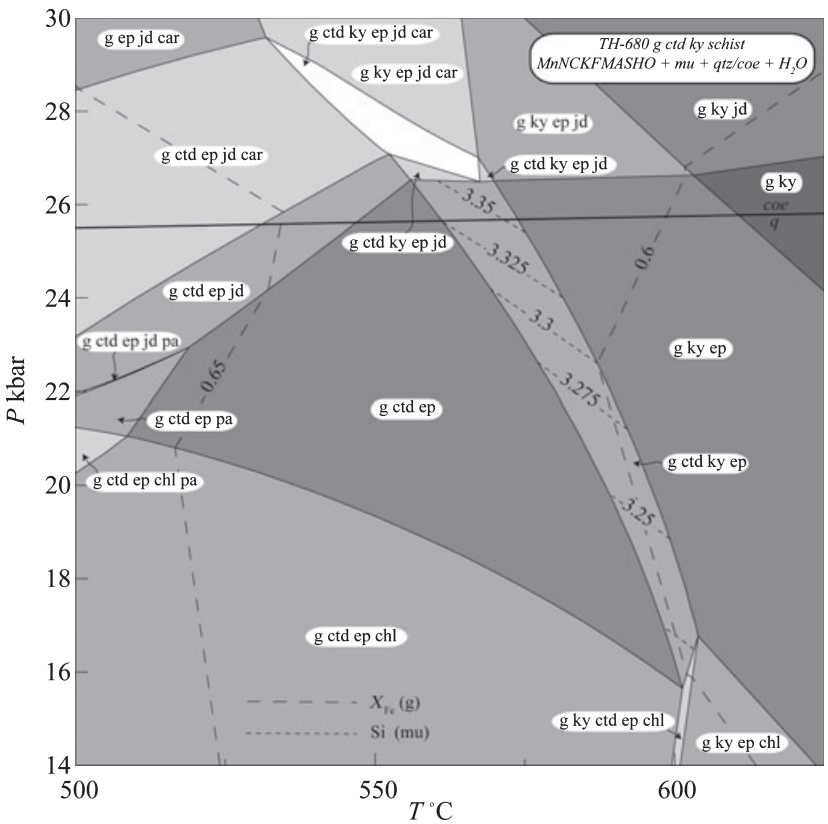

Fig. 5. MnNCKFMASHO pseudosection for rock TH-680. Bulk composition used: SiO_2, 70.31; Al_2O_3, 13.76; CaO, 1.29; MgO, 3.64; FeO, 6.53; MnO, 0.09; 6.53; K_2O, 3.53; Na_2O, 0.24; O, 0.70.

Manganese in epidote was ignored because only trace amounts of Mn are found in electron microprobe analyses of the TH-680 epidote. The principal effect of considering manganese in phase equilibria calculations is to extend the garnet stability field down temperature as described by Mahar *et al.* (1997) and thus the pseudosection is only rigorously applicable to the stages postdating initial garnet growth. Manganese addition to NCKFMASHO can be seen to extend the pressure range of the garnet–chloritoid–kyanite(±epidote) field to occupy the region 14–25 kbar and 550–610 °C.

Another pseudosection (Fig. 6) was also drawn for bulk composition ALM-45 from the Betics for comparison, and because this rock and its conditions of formation have not been described before. Immediately obvious is the very much enlarged field for the critical assemblage garnet–chloritoid–kyanite (±epidote). Paragonite is stabilized over a large range in *P–T* because of the higher Na_2O content of this rock, and the greatly extended garnet–chloritoid–kyanite field is largely due to the greater Al_2O_3:K_2O ratio relative to TH-680.

DISCUSSION

Bulk compositions

The series of *P–T* pseudosections for TH-680 show that sodium, calcium, ferric iron and manganese collectively expand the garnet–chloritoid–kyanite stability field from a thin (≈15 °C wide) field covering 8 kbar of *P–T* space within KFMASH, to a significant region of eclogite facies *P–T*, within the full MnNCKFMASHO system. Although the addition of extra components to KFMASH enlarges the field of garnet–chloritoid–kyanite, there are two further bulk compositional controls: the Al_2O_3:K_2O and FeO:MgO ratios of the rocks. Figure 7 shows the effect of varying Al_2O_3:K_2O on the size and position of TH-680's garnet–chloritoid–kyanite field whilst keeping other compositional parameters constant. If this ratio is small, there will be little Al_2O_3 left over, after making phengite, to produce much free kyanite. Likewise, larger values of this ratio will produce larger amounts of kyanite. Interestingly, at higher values of Al_2O_3:K_2O, the lower temperature boundary of the stability field is defined by the appearance of garnet at the expense of chloritoid and kyanite, as opposed to the reaction: chloritoid = garnet + kyanite + H_2O, present at lower values (< 5). The typical Dalradian pelite composition has a smaller ratio (4.33) and hence a very small *P–T* field for this assemblage, whereas the Betics rock ALM-45 has a large ratio (6.15) and a much larger stability field. Importantly, in the Dalradian bulk composition used in Coggon & Holland (2002) the Al_2O_3 content was adjusted downwards by removing Al_2O_3 assumed to be combined with Na_2O and CaO in plagioclase, further reducing the apparent Al_2O_3:K_2O ratio in KFMASH and hence in producing

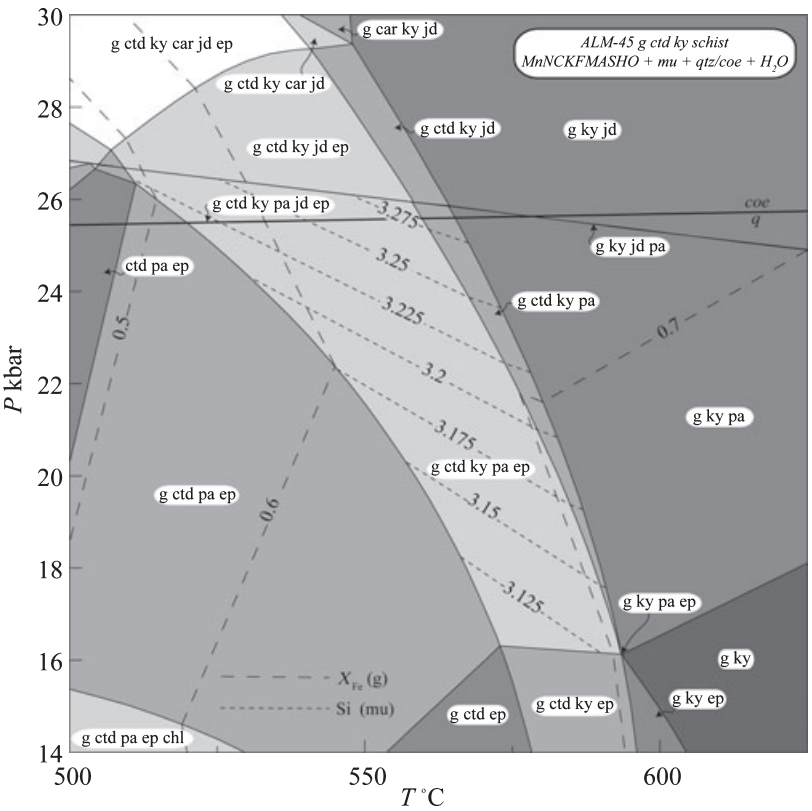

Fig. 6. MnNCKFMASHO pseudosection for rock ALM-45. Bulk composition used: SiO_2, 68.08; Al_2O_3, 16.30; CaO, 1.11; MgO, 2.34; FeO, 8.03; MnO, 0.28; K_2O, 2.65; Na_2O, 0.51; O, 0.70.

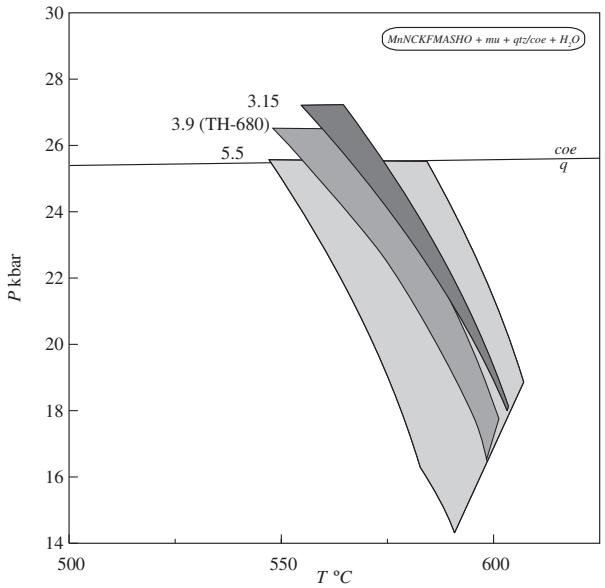

Fig. 7. Effect of variable Al_2O_3:K_2O ratio on the garnet–chloritoid–kyanite stability field using the bulk composition of TH-680. Numbers represent bulk Al_2O_3:K_2O ratio value.

the unreasonably small field for the critical assemblage in that paper. Although Al_2O_3:K_2O appears to be the dominant compositional control on stability field size, the rock's FeO:MgO ratio also has a considerable effect on field position and topology. Figure 8 illustrates this graphically by varying the bulk X_{Fe} number [FeO/(FeO + MgO)], of TH-680 with lower values shifting the field boundaries to higher temperatures

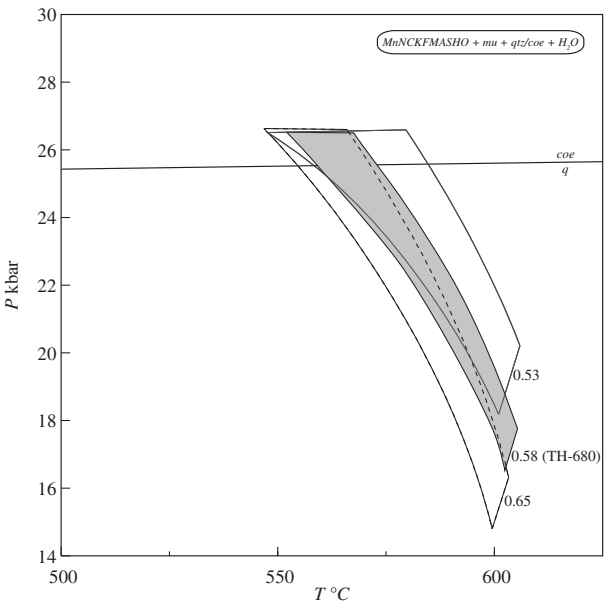

Fig. 8. Effect of variable FeO:MgO ratio on the garnet–chloritoid–kyanite stability field using the bulk composition of TH-680. Numbers represent bulk X_{Fe} [FeO/(FeO + MgO)] value.

and pressures. This is largely a result of increasing the clinochlore component of chlorite and the magnesium component of chloritoid, which then stabilizes chlorite and chloritoid to higher pressures and temperatures respectively. The AFM projection shown in Fig. 9 shows that all of the garnet–chloritoid–kyanite schists studied here, lie at lower values of FeO:MgO than the Dalradian pelite.

A comparison of the bulk-rock chemistry for several garnet–chloritoid–kyanite metapelites (Fig. 9; Table 1) collected from the Tauern Window, the Raspas Complex, Ecuador, the Carpathians and the Betics, respectively, shows that, relative to an average Dalradian pelite composition (Mahar *et al.*, 1997), all have lower or similar manganese contents. This demonstrates that the assemblage is not formed as a result of anomalously high-manganese bulk compositions, but

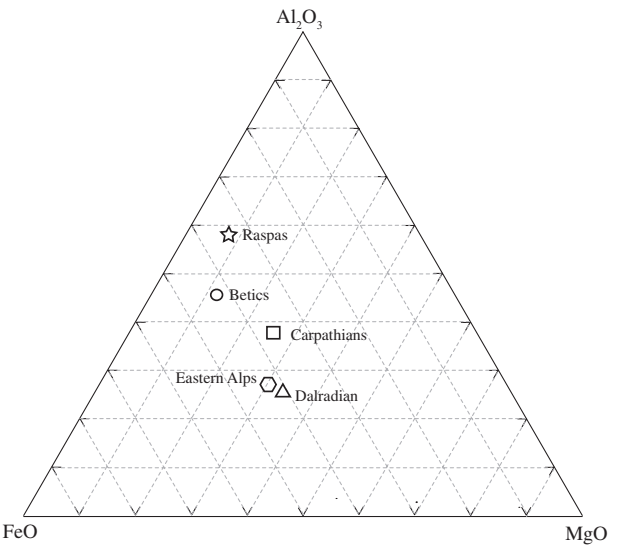

Fig. 9. Bulk-rock AFM projection from muscovite, quartz and H_2O, for a range of garnet–chloritoid–kyanite schists and a Dalradian pelite. Data are obtained from the following sources: Dalradian average pelite (triangle), Mahar *et al.* (1997); the Eastern Alps (hexagon), this study; the Carpathians (square), Negulescu *et al.* (2009); the Raspas complex (star), Gabriele *et al.* (2003); the Betics (ellipse), this study.

Table 1. Comparison of a suite of garnet–chloritoid–kyanite schist bulk compositions with a Dalradian average pelite.

	TH-680	Raspas	Carpathians	Betics	Dalradian
SiO_2	64.21	76.03	64.97	60.15	59.8
TiO_2	0.14	0.82	0.83	0.2	–
Al_2O_3	21.33	13.05	17.49	24.23	16.57
FeO	5.64	3.74	5.99	8.49	5.81
MnO	0.08	0.03	0.07	0.29	0.10
MgO	2.23	0.45	2.37	1.39	2.62
CaO	1.10	0.18	0.97	0.92	1.09
Na_2O	0.22	0.68	1.57	0.46	1.73
K_2O	5.05	1.31	2.64	3.67	3.53

Values are weight % oxide. TH-680: Tauern metapelite, this study; Raspas: Gabriele *et al.* (2003); Carpathians: Negulescu *et al.* (2009); Betics: ALM-45 metapelite, this study; Dalradian average pelite: Mahar *et al.* (1997).

Table 2. Representative electron microprobe analyses of major minerals from eclogite facies metasedimentary rocks of the Eastern Alps and the Betics.

	Eastern Alps: TH-680					Betics: ALM-45			
	$Garnet_{rim}$	$Garnet_{core}$	Chloritoid	Phengite	Epidote	$Garnet_{rim}$	$Garnet_{core}$	Chloritoid	Phengite
SiO_2	37.48	35.89	24.77	50.48	37.86	36.51	38.14	24.52	47.98
TiO_2	0.03	0.08	0.00	0.33	0.19	0.03	0.09	0.00	0.30
Al_2O_3	21.60	21.20	40.46	28.30	27.12	21.28	20.98	41.07	32.74
Cr_2O_3	0.00	0.00	0.02	0.02	0.01	0.01	0.00	0.00	0.01
FeO	29.19	30.93	19.17	1.97	6.37	37.57	31.52	21.01	1.28
MnO	0.07	0.76	0.27	0.02	0.04	0.27	2.05	0.04	0.00
MgO	4.39	3.27	6.11	3.40	0.31	3.85	2.05	4.93	0.18
CaO	7.23	6.41	0.02	0.02	21.74	0.73	5.74	0.04	0.00
Na_2O	0.03	0.06	0.01	0.36	0.04	0.13	0.16	0.05	0.15
K_2O	0.00	0.00	0.00	10.81	0.07	0.00	0.00	0.00	0.77
Total	100.02	98.60	90.83	95.76	93.75	100.43	99.94	91.69	94.47
No. of oxygen	12	12	6	11	12.5	12	12	6	11
Si	2.95	2.90	1.11	3.36	3.04	2.92	3.06	1.00	3.20
Ti	0.00	0.00	0.00	0.02	0.01	0.00	0.09	0.00	0.02
Al	2.00	2.00	1.87	2.22	2.57	2.00	1.98	1.98	2.58
Fe_{tot}	1.87	1.98	0.65	0.11	0.26	2.42	2.11	0.70	0.07
Mn	0.01	0.05	0.01	0.00	0.00	0.02	0.14	0.00	0.00
Mg	0.51	0.39	0.32	0.34	0.04	0.46	0.15	0.30	0.18
Ca	0.61	0.55	0.00	0.00	1.87	0.06	0.49	0.00	0.00
Na	0.01	0.01	0.00	0.05	0.01	0.02	0.03	0.00	0.15
K	0.00	0.00	0.00	0.92	0.01	0.00	0.00	0.00	0.77

that small amounts of manganese and ferric iron partitioning into garnet and chloritoid may stabilize the assemblage significantly. Similarly, these rocks are not particularly oxidized, having ferric iron contents comparable with those found in average pelitic compositions (White *et al.*, 2000). However, all of the schists have a higher Al_2O_3:K_2O ratio than the average Dalradian pelite.

Water activity is taken as unity for all thermobarometric and phase diagram calculations presented in this paper. At these pressures, although dissolved silicate material is expected to be significant, the solvus-like behaviour of silicate–water systems (e.g. Shen & Keppler (1997) implies extremely non-ideal solutions characterized by large activity coefficients such that even for high silicate concentrations the water activity will remain much larger than mole fraction. Holland (1979) showed that high water activity is valid in the Eclogite Zone of the Eastern Alps by measuring the composition of fluid inclusions in eclogitic omphacite and zoisite, and concluding that X_{CO_2} in the fluid was less than 0.1. This is also supported petrographically by the lack of a common carbonate phase in studied garnet–chloritoid–kyanite schists. Modelling with a reduced water activity of 0.8 applied to these pseudosections and thermobarometric calculations shows that temperatures of critical boundaries and *P–T* estimates only decrease by 15–20 °C – a value within the likely error of the calculations.

Comparison of peak *P–T* conditions

In order to assess the range and similarity in peak metamorphic conditions experienced by the garnet–chloritoid–kyanite schists described above, the results of a comparative average *P–T* study performed are presented using the av*PT* mode of THERMOCALC version 3.33 (Holland & Powell, 1998). Mineral data from phase constituents of peak eclogite facies mineral assemblages were taken from both literature sources and freshly obtained electron microprobe data sets (Table 2). Recalculation of mineral analyses into end-member activities and the estimation of Fe^{3+} iron quantities was performed using the software AX which is downloadable from http://www.esc.cam.ac.uk/research/research-groups/holland/ax.

All calculations used reactions 1–4 of the following equilibria. Reaction 5 was also used in TH-680 because it contained additional clinozoisite.

1. 3mctd + 2q = py + 2ky + $3H_2O$
2. 3fctd + 2q = alm + 2ky + $3H_2O$
3. 3cel + 4ky = py + 3mu + 4q
4. 3fcel + 4ky = alm + 3mu + 4q
5. 6cz = 4gr + q + 5ky + $3H_2O$

Average *P–T* calculations were applied to all sample areas described above except for the Kokchetav Massif due to a lack of suitable mineral data for comparison. *P–T* estimates and associated error ellipses are presented in Table 3 and Fig. 10 respectively. For consistency, the same set of independent reactions

Table 3. Results of average *P–T* calculations.

	Sample	Assemblage	P	σ_P	T	σ_T	σ_{fit}
Eastern Alps	TH-680[a]	g ctd ky mu q ep	26.2	1.8	553	12	1.13
Carpathians	RU007[b]	g ctd ky mu q	24.6	1.8	590	12	0.67
Western Alps	Unspecified[c]	g ctd ky mu q	29.9	2.7	544	18	1.63
Andes	98RR11, 97Ce5[d]	g ctd ky mu q	20.3	2.8	569	14	1.42
Bohemian Massif	HH-1[e]	g ctd ky mu q	27.2	2.7	546	16	1.44
Betics	ALM-45[f]	g ctd ky mu q	20.8	2.0	580	10	0.81

[a]This study.
[b]Negulescu *et al.* (2009).
[c]Zucali *et al.* (2002).
[d]Gabriele *et al.* (2003).
[e]Konopasek (2001).
[f]This study.

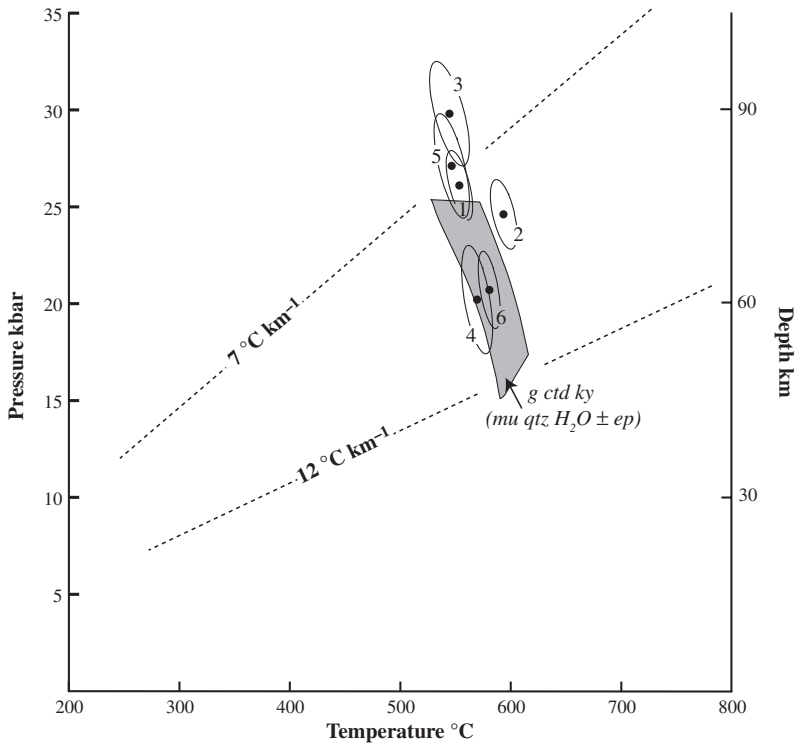

Fig. 10. Comparison of average *P–T* estimates. Note the restricted temperature interval within which all estimates reside. Error ellipses are 1σ width. Ellipses are numbered as follows: 1 = Eastern Alps, 2 = Carpathians, 3 = Western Alps, 4 = Andes, 5 = Bohemian Massif, 6 = Betics.

was used calculations, a_{H_2O} was set at unity and 5% of total iron in muscovite was taken as Fe_2O_3.

Average pressures and temperatures cluster in two distinct groups separated by differences in pressure. Critically, constraints associated with pressure estimates are poor relative to temperature constraints. This is due to the small values of ΔV involved in equilibria devoid of garnet and plagioclase and is a problem inherent to any calculation of pressure from eclogite facies rocks. Fit parameters for all calculations lie within the 95% confidence interval (i.e. ≤1.73 for four reactions or ≤1.61 for five reactions). Samples 98RR11 and ALM-45 from the Bohemian Massif and the Andes, respectively, yield similar peak conditions ~20.5 kbar at 570–80 °C and are the lowest pressure rocks of all samples studied. Although similar in temperature, the pressure estimates for samples from both the Eastern and Western Alps and the Bohemian Massif are significantly higher than in the other localities. Interestingly, these estimates lie within the coesite stability field, and yet coesite is yet to be reported from any of these localities. Calculations based on mineral data presented by Zucali *et al.* (2002) for the Sesia zone eclogitic micaschists produce the highest pressures reported in this study. However, it is doubtful whether analyses presented in Zucali *et al.* (2002) and employed in the calculation are from the same rock and hence the resultant estimate is approximate at best. Sample RU007 from the Carpathians yields an average *P–T* estimate of 24.6 kbar and 590 °C, between the clusters. Importantly, with the exception of RU007, all *P–T* estimates lie within 40 °C of each other, between 540 and 590 °C. Despite the variation in pressures between samples, peak temperature estimates are better constrained and lie within a narrowly restricted range. This is surprising given the range of bulk compositions, in particular Al_2O_3:K_2O ratios (Fig. 9), between the schists and suggests that the peak temperature attained during subduction may be a critical factor affecting the depth of the subduction–exhumation transition.

Tectonic significance

It is very curious that such a large number of eclogite facies rocks from oceanic crust and passive margin sequences, both pelitic garnet–chloritoid–kyanite-bearing schists as shown here and also mafic eclogites, seem to record maximum conditions of subduction within the restricted temperature range 550–600 °C at 23 ± 3 kbar (for a review, see Zucali *et al.*, 2002). The following discussion addresses specifically the subduction of rheologically weak oceanic and shelf material and does not address the separate problem of ultra-high-pressure terranes.

Average *P–T* calculations presented above suggest that thermal grade is a more critical parameter than pressure of subduction. The implication is that subduction tectonics require the down-going margin slab top, where both mafic and sedimentary protoliths may coexist, to pass through a *P–T* window in the region of 60–75 km depth at temperatures of 550–600 °C, within which eclogite facies units are decoupled from the slab and subsequently exhumed. Variations in subduction

zone geothermal gradient mean that the slab top will reach the critical temperature range at different depths, hence the spread of pressure values between 550 and 600 °C in Fig. 10. As evidenced by the relatively uncommon nature of UHP terranes, rocks which are subducted to higher grade are seldom returned to the surface and if so, are commonly metamorphosed portions of rheologically strong, buoyant continental basement, e.g. Dora Maira massif, Western Alps (Chopin *et al.*, 1991).

The question of what critically controls the subduction–exhumation transition in portions of transitional crust has been approached in several petrographical and experimental studies. Stöckhert *et al.* (1997) investigated the microstructure of quartz in eclogite facies garnet–chloritoid–kyanite micaschists of the Tauern window and suggested that the mechanism of quartz deformation changed from being controlled by grain boundary free energy during peak pressure conditions at low deviatoric stress values, to the regime of dislocation creep during the early stages of exhumation. Their well-constrained *P–T* path shows that the critical assemblage was stable through late stages of subduction and early stages of exhumation, i.e. through the period of detachment from the slab top. This is also reported by Gabriele *et al.* (2003) in garnet–chloritoid–kyanite bearing schists of the Raspas complex, Andes. Together with the thermobarometric work of this study, this points towards garnet–chloritoid–kyanite assemblages in aluminous metapelites as representing an enhanced detachment state of subducted material.

Several authors point towards the importance of an interplate shear zone which migrates toward zones of lower rheological strength during subduction (Peacock, 1992, 1996; Stöckhert *et al.*, 1997). The lateral shift of a weak zone from the plate interface into footwall units would decouple slab top material from the slab if buoyancy forces are greater than viscous drag forces associated with subduction (e.g. England & Holland (1979). More recently Jolivet *et al.* (2005) proposed that decoupling of eclogite units from the slab occurs as a result of the progressive formation of shear zones synchronous with eclogitization and associated drop in rock strength. Although their study focuses on the Bergen Arc eclogite terrane – a type example of continental subduction and therefore outside the focus of this study, the processes operating in and proximal to the slab top during the subduction–exhumation transition are likely to be applicable to subduction of passive margins. They show how a gradual succession from brittle fracturing, fluid infiltration and recrystallization leads to localization of strain in ductile shear zones and eventual decoupling of units along such zones. Rheologically weaker material would decouple from the slab top at lower threshold values than those experienced by the Bergen eclogites. This hypothesis is consistent with the 2D numerical modelling study of Carry *et al.* (2009), which points to the development of two separate strength gradients

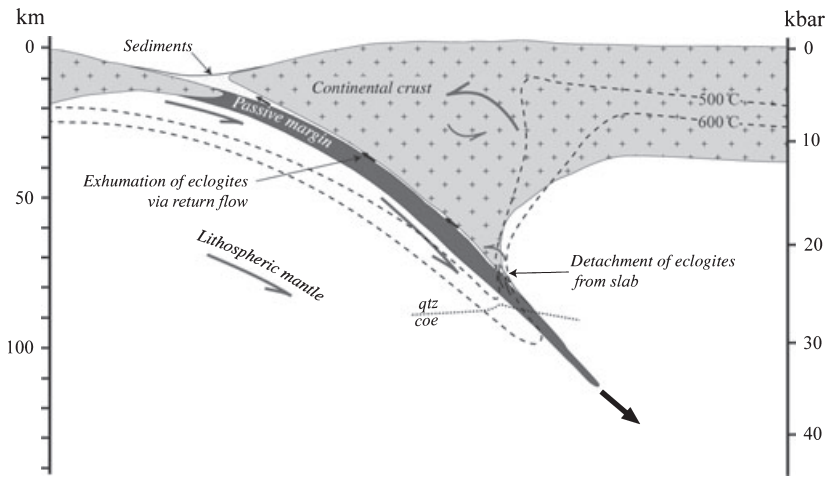

Fig. 11. Schematic showing tectonic setting for the exhumation of eclogites from a subducted continental margin. Isotherms and associated kinematic indicators taken from Gerya & Stöckhert (2006) (model HYAA – 15 Ma post subduction initiation) delineate the thermal weakening threshold where detachment of material from the slab occurs.

Table 4. Comparison of tectonic settings for garnet–chloritoid–kyanite schist localities.

Locality	Setting	References
Eastern Alps	Passive margin sequence	Holland (1979) and Kurz *et al.* (1998, 1999)
Western Alps	Austroalpine continental margin	Stella (1894), Dal Piaz *et al.* (1972), Compagnoni (1977), Compagnoni *et al.* (1977) and Tropper *et al.* (1999)
Carpathians	Subduction melange complex	Balintoni *et al.* (2009), Negulescu *et al.* (2009) and Sabau (2000)
Andes	Composite fragment of oceanic lithosphere	Feininger (1980), Gabriele (2002) and Gabriele *et al.* (2003)
Bohemian Massif	Passive margin sequence	Hofmann *et al.* (1988), Krohe (1996) and Konopasek (2001)
Betics	Passive margin sequence	Akkerman *et al.* (1980), Weijermars (1991) and Jolivet *et al.* (2003)

evolving within the slab during subduction: one parallel to the length of the slab where the ductile strength decreases with depth and a second one normal to the slab where the ductile strength increases with depth as a result of the slab's temperature distribution. They conclude that detachment of individual *HP–LT* units occurs when the strength of the subducted slab becomes lower than the applied net stress. Importantly, Carry *et al*. (2009), along with the earlier work of den Beukel (1992), showed that thermal weakening of the slab top is a critical control on when detachment occurs.

We find that the recent thermomechanical modelling studies of active continental margins of Stöckhert & Gerya (2005) and Gerya & Stöckhert (2006) produce decompressive *P–T* paths for slab top material which support the common 550–600 °C and 23 ± 3 kbar subduction maximum discussed above (see Fig. 11). Commonly such models predict peak temperatures which are cooler than those deduced from thermobarometry. Importantly, peak temperature attained within the slab top is largely affected by convergence rate. The results of this study should help constrain such models by fixing the depths and temperatures where detachment of the crustal units occurs.

Thus, it appears that the strength of the subducted lithosphere is the critical factor in determining the transition from subduction to exhumation of *HP* material. A comparison of protolith environments for the garnet–chloritoid–kyanite schists discussed above, shows that such rocks are commonly associated with mafic eclogites and interpreted as representing supracrustal passive margin sequences (see Table 4). Given the coexistence of similar lithologies, it is likely that the net strength, resultant from a number of variables including crustal thickness, subduction angle, convergence rate and thermal architecture, will be comparable across a wide range of collisional settings.

CONCLUSION

The assemblage garnet–chloritoid–kyanite has been shown to be a key eclogite facies paragenesis. Despite being heavily favoured by bulk compositions with high Al_2O_3:K_2O ratios, the assemblage is stable over a restricted range of eclogite facies *P–T* space. Average *P–T* calculations show that the assemblage forms in a narrow temperature interval between 540 and 590 °C at pressures of 23 ± 3 kbar in the eclogite facies. This, in addition to reported *P–T* estimates from mafic eclogites, supports the conclusion that a thermal threshold exists for subducted slab top material, beyond which material is rarely exhumed. Thermal weakening of the slab must, therefore, play a critical role in the subduction–exhumation transition where buoyancy (thermal expansion) forces become greater than viscous slab pull forces associated with the subduction of oceanic lithosphere. Data presented in this study provide an important calibration for theoretical models of active continental margins.

ACKNOWLEDGEMENTS

A. J. S. acknowledges support of a NERC postgraduate studentship. T. Gerya (ETHZ), J. Butler (Dalhousie) and C. Warren (Open University) are thanked for helpful and stimulating discussion regarding geodynamic modelling. We gratefully acknowledge formal reviews of the manuscript by P. Agard and an anonymous reviewer, which improved the paper. Mineral analyses were obtained using the Department of Earth Sciences' electron microprobe under the careful guidance of C. Petrone. K. Gray provided invaluable support in the construction of thin sections.

REFERENCES

Ackermand, D. & Morteani, G., 1973. Occurrence and breakdown of paragonite and margarite in the Greiner Schiefer series (Zillerthal Alps, Tyrol). *Contributions to Mineralogy and Petrology*, **40,** 293–304.

Agard, P., Yamato, P., Jolivet, L. & Burov, E., 2009. Exhumation of oceanic blueschists and eclogites in subduction zones: timing and mechanisms. *Earth Science Reviews*, **92,** 53–79.

Akkerman, J., Maier, G. & Simon, O., 1980. On the geology of the Alpujarride Complex in the western Sierra de las Estancias (Betic Cordilleras, SE Spain). *Geologie en Mijnbouw*, **59,** 363–374.

Arculus, R., Lapierre, H. & Jaillard, E., 1999. Geochemical window into subduction and accretion processes: Raspas Metamorphic Complex, Ecuador. *Geology*, **27,** 547.

Balintoni, I., Balica, C., Ducea, M., Chen, F., Hann, H. & Sabliovschi, V., 2009. Late Cambrian–Early Ordovician Gondwanan terranes in the Romanian Carpathians: a zircon U–Pb provenance study. *Gondwana Research*, **16,** 119–133.

Baltatzis, E. & Katagas, C., 1981. Margarite pseudomorphs after kyanite in Glen Esk, Scotland. *American Mineralogist*, **66,** 213–216.

den Beukel, J., 1992. Some thermomechanical aspects of the subduction of continental lithosphere. *Tectonics*, **11,** 316–329.

Bucher-Nurminen, K., Frank, E. & Frey, M., 1983. A model for the progressive regional metamorphism of margarite-bearing rocks in the central Alps. *American Journal of Science*, **283,** 370–395.

Carry, N., Gueydan, F., Brun, J. & Marquer, D., 2009. Mechanical decoupling of high-pressure crustal units during continental subduction. *Earth and Planetary Science Letters*, **278,** 13–25.

Chauvet, A., Kienast, J., Pinardon, J. & Brunel, M., 1992. Petrological constraints and PT path of Devonian collapse tectonics within the Scandian mountain belt (Western Gneiss Region, Norway). *Journal of the Geological Society*, **149,** 383–400.

Chopin, C., Henry, C. & Michard, A., 1991. Geology and petrology of the coesite-bearing terrain, Dora Maira massif, Western Alps. *European Journal of Mineralogy*, **3,** 263–291.

Coggon, R. & Holland, T., 2002. Mixing properties of phengitic micas and revised garnet–phengite thermobarometers. *Journal of Metamorphic Geology*, **20,** 683–696.

Compagnoni, R., 1977. The Sesia–Lanzo Zone: high pressure–low temperature metamorphism in the Austroalpine continental margin. *Rendiconti della Societa Italiana di Mineralogia e Petrologia*, **33,** 335–374.

Compagnoni, R., Dal Piaz, G., Hunziker, J., Gosso, G., Lombardo, B. & Williams, P., 1977. The Sesia–Lanzo zone, a slice of continental crust with Alpine high pressure–low temperature assemblages in the Western Italian Alps. *Rendiconti della Societa Italiana di Mineralogia e Petrologia*, **33,** 335–374.

Dal Piaz, G., Hunziker, J. & Martinotti, G., 1972. La zona Sesia–Lanzo e l'evoluzione tettonico-metamorfca delle Alpi

nordoccidentali interne. *Memorie della Società Geologica Italiana*, **11,** 433–466.
Dale, J. & Holland, T.J.B., 2003. Geothermobarometry, *P–T* paths and metamorphic field gradients of high-pressure rocks from the Adula Nappe, Central Alps. *Journal of Metamorphic Geology*, **21,** 813–829.
Duchêne, S. *et al*., 1997. The lu–hf dating of garnets and the ages of the alpine high-pressure metamorphism. *Nature*, **387,** 586–589.
Dyar, M.D., Lowe, E.W., Guidotti, C.V. & Delaney, J.S., 2002. Fe^{3+} and Fe^{2+} partitioning among silicates in metapelites: a synchrotron micro-XANES study. *American Mineralogist*, **87,** 514–522.
England, P. & Holland, T., 1979. Archimedes and the Tauern eclogites: the role of buoyancy in the preservation of exotic eclogite blocks. *Earth and Planetary Science Letters*, **44,** 287–294.
Feenstra, A., 1996. An EMP and TEM–AEM study of margarite, muscovite and paragonite in polymetamorphic metabauxites of Naxos Cyclades, Greece) and the implications of fine-scale mica interlayering and multiple mica generations. *Journal of Petrology*, **37,** 201–233.
Feininger, T., 1980. Eclogite and related high-pressure regional metamorphic rocks from the Andes of Ecuador. *Journal of Petrology*, **21,** 107–140.
Feininger, T. & Silberman, M., 1982. K–Ar geochronology of basement rocks on the Northern Flank of the Huancabamba de ection, Ecuador. Open-File Report – US Geological Survey, pp. 82–206.
Franz, G., Hinrichsen, T. & Wannemacher, E., 1977. Determination of the miscibility gap on the solid solution series paragonite–margarite by means of the infrared spectroscopy. *Contributions to Mineralogy and Petrology*, **59,** 307–316.
Gabriele, P., 2002. HP terranes exhumation in an active margin setting. *Geology, Petrology and Geochemistry of the Raspas Complex in SW Ecuador*. PhD Thesis, Université de Lausanne, Faculté des géoscience et de l environnement, Abstract: http://www.unil.ch/jahia/site/gse/cache/off/lang/en/pid/9506.
Gabriele, P., Ballevre, M., Jaillard, E. & Hernandez, J., 2003. Garnet–chloritoid–kyanite metapelites from the Raspas Complex (SW Ecuador): a key eclogite-facies assemblage. *European Journal of Mineralogy*, **15,** 977–989.
Gerya, T. & Stöckhert, B., 2006. Two-dimensional numerical modeling of tectonic and metamorphic histories at active continental margins. *International Journal of Earth Sciences*, **95,** 250–274.
Guidotti, C. & Cheney, J., 1976. Margarite pseudomorphs after chiastolite in the Rangeley area, Maine. *American Mineralogist*, **61,** 431–434.
Guidotti, C., Post, J. & Cheney, J., 1979. Margarite pseudomorphs after chiastolite in the Georgetown area, California. *American Mineralogist*, **64,** 728–732.
Hacker, B., Andersen, T., Root, D., Mehl, L., Mattinson, J. & Wooden, J., 2003. Exhumation of high-pressure rocks beneath the Solund Basin, Western Gneiss Region of Norway. *Journal of Metamorphic Geology*, **21,** 613–629.
Harte, B., 1975. Determination of a pelite petrogenetic grid for the determination of a pelite petrogenetic grid for the eastern Scottish Dalradian. *Yearbook of the Carnegie Institution of Washington*, **74,** 438–446.
Harte, B. & Hudson, N.F.C., 1979. Pelite facies series and the temperatures and pressures of Dalradian metamorphism in eastern Scotland. In: *The Caledonides of the British Isles Reviewed* (eds Harris, A.L., Holland, C.H. & Leake, B.E.), *Geology Society Special Publication London*, **8,** 323–337.
Hermann, J., 2002. Experimental constraints on phase relations in subducted continental crust. *Contributions to Mineralogy and Petrology*, **143,** 219–235.
Hinrichsen, T. & Schurmann, K., 1971. Synthese und Stabilität von Glimmern im System $CaO–Na_2O–Al_2O_3–SiO_2–H_2O$. *Fortschritte der Mineralogie*, **49,** 21.
Höck, V., 1974. Coexisting phengite, paragonite and margarite in metasediments of the Mittlere Hohe Tauern, Austria. *Contributions to Mineralogy and Petrology*, **43,** 261–273.
Hofmann, J., Mathé, G. & Werner, C., 1988. Saxothuringian zone and the central German crystalline zone in the German Democratic Republik. *Precambrian in Younger Fold Belts. European Variscides, the Carpathians and Balkans* (ed. Zoubek, V.), Wiley and Sons, 119–144.
Holland, T., 1979. High water activities in the generation of high pressure kyanite eclogites of the Tauern Window, Austria. *Journal of Geology*, **87,** 27.
Holland, T. & Powell, R., 1990. An enlarged and updated internally consistent thermodynamic dataset with uncertainties and correlations: the system $K_2O–Na_2O–CaO–MgO–MnO–FeO–Fe_2O_3–Al_2O_3–TiO_2–SiO_2–C–H_2–O_2$. *Journal of Metamorphic Geology*, **8,** 89–124.
Holland, T. & Powell, R., 1998. An internally consistent thermodynamic data set for phases of petrological interest. *Journal of Metamorphic Geology*, **16,** 309–343.
Holland, T. & Powell, R., 2003. Activity–composition relations for phases in petrological calculations: an asymmetric multicomponent formulation. *Contributions to Mineralogy and Petrology*, **145,** 492–501.
Holland, T., Baker, J. & Powell, R., 1998. Mixing properties and activity-composition relationships of chlorites in the system $MgO–FeO–Al_2O_3–SiO_2–H_2O$. *European Journal of Mineralogy*, **10,** 395–406.
Jaillard, E., Soler, P., Carlier, G. & Mourier, T., 1990. Geodynamic evolution of the northern and central andes during early to middle mesozoic times: a Tethyan model. *Journal of the Geological Society*, **147,** 1009–1022.
Jolivet, L., Faccenna, C., Goffe, B., Burov, E. & Agard, P., 2003. Subduction tectonics and exhumation of high-pressure metamorphic rocks in the Mediterranean orogens. *American Journal of Science*, **303,** 353–409.
Jolivet, L., Raimbourg, H., Labrousse, L. *et al*., 2005. Softening triggered by eclogitization, the first step toward exhumation during continental subduction. *Earth and Planetary Science Letters*, **237,** 532–547.
Keller, L., De Capitani, C. & Abart, R., 2005. A quaternary solution model for white micas based on natural coexisting phengite–paragonite Pairs. *Journal of Petrology*, **46,** 2129–2144.
Konopasek, J., 2001. Eclogitic micaschists in the central part of the Krusne Hory Mountains (Bohemian Massif). *European Journal of Mineralogy*, **13,** 87–100.
Krohe, A., 1996. Variscan tectonics of central Europe: postaccretionary intraplate deformation of weak continental lithosphere. *Tectonics*, **15,** 1364–1388.
Kurz, W., Neubauer, F., Genser, J. & Dachs, E., 1998. Alpine geodynamic evolution of passive and active continental margin sequences in the Tauern Window (eastern Alps, Austria, Italy): a review. *Geologische Rundschau*, **87,** 225–242.
Kurz, W., Neubauer, F. & Unzog, W., 1999. Evolution of Alpine eclogites in the Eastern Alps: implications for Alpine geodynamics. *Physics and Chemistry of the Earth, Part A*, **24,** 667–674.
Leech, M., Singh, S., Jain, A., Klemperer, S. & Manickavasagam, R., 2005. The onset of India–Asia continental collision: early, steep subduction required by the timing of UHP metamorphism in the Western Himalaya. *Earth and Planetary Science Letters*, **234,** 83–97.
Mahar, E., Baker, J., Powell, R., Holland, T. & Howell, N., 1997. The effect of Mn on mineral stability in metapelites. *Journal of Metamorphic Geology*, **15,** 223–238.
Massonne, H., 2000. Experimental aspects of UHP metamorphism in pelitic systems. *Ultrahigh-Pressure Metamorphism and Geodynamics in Collision-Type Orogenic Belts: Final Report of the Task Group III-6 (1994–1998) of the International Lithosphere Project*, 105 pp.
Massonne, H. & Schreyer, W., 1989. Stability field of the high-pressure assemblage, talc + phengite and two new phengite barometers. *European Journal of Mineralogy*, **1,** 391–410.

Meyre, C., De Capitani, C., Zack, T. & Frey, M., 1999. Petrology of high-pressure metapelites from the Adula nappe (Central Alps, Switzerland). *Journal of Petrology*, **40,** 199–213.
Miller, C., 1977. Mineral parageneses recording the *PT* history of the alpine eclogites in the Tauern Window, Austria. *Neues Jahrbuch fur Minealogie, Abhandlungen*, **130,** 69–77.
Miller, C., Satir, M. & Frank, W., 1980. High pressure metamorphism in the Tauern Window. *Mitteilungen der Österreichischen Geologischen Gesellschaft*, **71,** 89–97.
Negulescu, E., Sabau, G. & Massonne, H., 2009. Chloritoid-bearing mineral assemblages in high-pressure metapelites from the Bughea Complex, Leaota Massif (South Carpathians). *Journal of Petrology*, **50,** 103.
Okuyama-Kusunose, Y., 1985. Margarite–paragonite–muscovite assemblages from the low-grade metapelites of the Tono metamorphic aureole, Kitakami Mountains, northeast Japan. *Ganseki Kobutsu Kosho Gakkaishi*, **80,** 515–525.
Parrish, R., Gough, S., Searle, M. & Waters, D., 2006. Plate velocity exhumation of ultrahigh-pressure eclogites in the Pakistan Himalaya. *Geology*, **34,** 989–992.
Peacock, S., 1992. Blueschist-facies metamorphism, shear heating, and *PTt* paths in subduction shear zones. *Journal of Geophysical Research-Solid Earth*, **97,** 17693–17707.
Peacock, S., 1996. Thermal and petrologic structure of subduction zones. *Geophysical Monograph*, **96,** 119–133.
Powell, R., 1987. Darken's quadratic formalism and the thermodynamics of minerals. *American Mineralogist*, **72,** 1–11.
Powell, R. & Holland, T.J.B., 1990. Calculated mineral equilibria in the pelite system, KFMASH (K_2O–FeO–MgO–Al_2O_3–SiO_2–H_2O). *American Mineralogist*, **75,** 367–380.
Rubatto, D. & Hermann, J., 2001. Exhumation as fast as subduction? *Geology*, **29,** 3–6.
Sabau, G., 2000. A possible UHP-eclogite in the Leaota Mts. (South Carpathians) and its history from high-pressure melting to retrograde inclusion in a subduction melange. *Lithos*, **52,** 253–276.
Schreyer, W., 1988. Experimental studies on metamorphism of crustal rocks under mantle pressures. *Mineralogical Magazine*, **52,** 1–26.
Searle, M., Waters, D., Martin, H. & Rex, D., 1994. Structure and metamorphism of blueschist–eclogite facies rocks from the northeastern Oman Mountains. *Journal of the Geological Society*, **151,** 555–576.
Searle, M., Warren, C., Waters, D. & Parrish, R., 2004. Structural evolution, metamorphism and restoration of the Arabian continental margin, Saih Hatat region, Oman Mountains. *Journal of Structural Geology*, **26,** 451–473.
Shen, A.H. & Keppler, H., 1997. Direct observation of completemiscibility in the albite–H_2O system. *Nature*, **385,** 710–712.
Sigoyer, J., Chavagnac, V., Blichert-Toft, J. *et al*., 2000. Dating the Indian continental subduction and collisional thickening in the Northwest Himalaya: multichronology of the Tso Morari eclogites. *Geology*, **28,** 487–490.
Spear, F. & Franz, G., 1986. *PT* evolution of metasediments from the Eclogite Zone, south-central Tauern Window, Austria. *Lithos*, **19,** 219–234.
Stella, A., 1894. Relazione sul rilevamento eseguito nell'anno 1893 nelle alpi occidentali (valli dell'orco e della soana). *Bolletino del Reale Comitato Geologica d'Italia*, **25,** 343–371.
Stöckhert, B. & Gerya, T., 2005. Pre-collisional high pressure metamorphism and nappe tectonics at active continental margins: a numerical simulation. *Terra Nova*, **17,** 102–110.
Stöckhert, B., Massonne, H. & Nowlan, E., 1997. Low differential stress during high-pressure metamorphism: the microstructural record of a metapelite from the Eclogite Zone, Tauern Window, Eastern Alps. *Lithos*, **41,** 103–108.
Tropper, P., Essene, E., Sharp, Z. & Hunziker, J., 1999. Application of K–feldspar–jadeite–quartz barometry to eclogite facies metagranites and metapelites in the Sesia Lanzo Zone (Western Alps, Italy). *Journal of Metamorphic Geology*, **17,** 195–210.
Udovkina, N., Muravitskaya, G. & Laputina, I., 1977. Talc–garnet–kyanite rocks of the Kokchetav block, northern Kazakhstan. *Doklady Akad Nauk SSSR*, **237,** 202–205.
Vuichard, J. & Ballevre, M., 1988. Garnet–chloritoid equilibria in eclogitic pelitic rocks from the Sesia zone (Western Alps): their bearing on phase relations in high pressure metapelites. *Journal of Metamorphic Geology*, **6,** 135–157.
Warren, C., Parrish, R., Searle, M. & Waters, D., 2003. Dating the subduction of the Arabian continental margin beneath the Semail Ophiolite, Oman. *Geology*, **31,** 889–892.
Wei, C. & Powell, R., 2003. Phase relations in high-pressure metapelites in the system KFMASH(K_2O–FeO–MgO–Al_2O_3–SiO_2–H_2O) with application to natural rocks. *Contributions to Mineralogy and Petrology*, **145,** 301–315.
Wei, C. & Powell, R., 2006. Calculated phase relations in the system NCKFMASH (Na_2O–CaO–K_2O–FeO–MgO–Al_2O_3–SiO_2–H_2O) for high-pressure metapelites. *Journal of Petrology*, **47,** 385–408.
Weijermars, R., 1991. Geology and tectonics of the Betic Zone, SE Spain. *Earth-Science Reviews*, **31,** 153–184.
White, R., Powell, R., Holland, T. & Worley, B., 2000. The effect of TiO_2 and Fe_2O_3 on metapelitic assemblages at greenschist and amphibolite facies conditions: mineral equilibria calculations in the system K_2O–FeO–MgO–Al_2O_3–SiO_2–H_2O–TiO_2–Fe_2O_3. *Journal of Metamorphic Geology*, **18,** 497–511.
White, R., Pomroy, N. & Powell, R., 2005. An *in-situ* metatexite–diatexite transition in upper amphibolite facies rocks from Broken Hill, Australia. *Journal of Metamorphic Geology*, **23,** 579–602.
Zucali, M., Spalla, M. & Gosso, G., 2002. Strain partitioning and fabric evolution as a correlation tool: the example of the Eclogitic Micaschists Complex in the Sesia–Lanzo Zone (Monte Mucrone–Monte Mars, Western Alps, Italy). *Schweizerische Mineralogische und Petrographische Mitteilungen*, **82,** 429–454.

APPENDIX: ACTIVITY MODELS USED IN CALCULATIONS

For white mica: activities are given by:

$$a_{\mathrm{mu}} = X_{\mathrm{K\ A}} X_{\mathrm{Al\ M2A}} X_{\mathrm{Al\ M2B}} X_{\mathrm{Si\ T1}} X_{\mathrm{Al\ T1}} \gamma_{\mathrm{mu}}$$

$$a_{\mathrm{cel}} = X_{\mathrm{K\ A}} X_{\mathrm{Mg\ M2A}} X_{\mathrm{Al\ M2B}} X^2_{\mathrm{Si\ T1}} \gamma_{\mathrm{cel}}$$

$$a_{\mathrm{fcel}} = X_{\mathrm{K\ A}} X_{\mathrm{Fe\ M2A}} X_{\mathrm{Al\ M2B}} X^2_{\mathrm{Si\ T1}} \gamma_{\mathrm{fcel}}$$

$$a_{\mathrm{pa}} = X_{\mathrm{Na\ A}} X_{\mathrm{Al\ M2A}} X_{\mathrm{Al\ M2B}} X_{\mathrm{Si\ T1}} X_{\mathrm{Al\ T1}} \gamma_{\mathrm{mu}}$$

$$a_{\mathrm{ma}} = X_{\mathrm{Ca\ A}} X_{\mathrm{Al\ M2A}} X_{\mathrm{Al\ M2B}} X^2_{\mathrm{Al\ T1}} \gamma_{\mathrm{ma}}$$

$$a_{\mathrm{fmu}} = X_{\mathrm{K\ A}} X_{\mathrm{Al\ M2A}} X_{\mathrm{Fe^{3+}\ M2B}} X_{\mathrm{Si\ T1}} X_{\mathrm{Al\ T1}} \gamma_{\mathrm{fmu}}$$

where the mixing energies for paragonite and muscovite are given by:

$$W_{\mathrm{mu.cel}} = 0 + 0.2P$$

$$W_{\mathrm{mu.fcel}} = 0 + 0.2P$$

$$W_{\mathrm{mu.pa}} = 10.12 + 0.0034T + 0.353P$$

$$W_{\mathrm{mu.ma}} = 35$$

$$W_{\text{mu.fmu}} = 0$$

$$W_{\text{cel.fcel}} = 0$$

$$W_{\text{cel.pa}} = 45 + 0.25P$$

$$W_{\text{cel.ma}} = 40$$

$$W_{\text{cel.fmu}} = 0$$

$$W_{\text{fcel.pa}} = 45 + 0.25P$$

$$W_{\text{fcel.ma}} = 40$$

$$W_{\text{fcel.fmu}} = 0$$

$$W_{\text{pa.ma}} = 15$$

$$W_{\text{pa.fmu}} = 30$$

$$W_{\text{ma.fmu}} = 35$$

Model mixing parameters for margarite are identical to the above except that $W_{\text{pa.ma}} = 13$ kJ.

The asymmetry parameters and DQF values (δ, Gibbs energy increments) for all end-members in muscovite and paragonite are:

	α	δ
mu	0.63	
cel	0.63	
fcel	0.63	
pa	0.37	
ma	0.63	1.7
fmu	0.63	30

and similarly for margarite

	α	δ
mu	0.63	1.0
cel	0.63	1.0
fcel	0.63	1.0
pa	0.37	1.2
ma	0.63	3.0
fmu	0.63	30

The Gibbs energy of fmu is taken to be that of mu + $\frac{1}{2}$hem − $\frac{1}{2}$cor + δ, with δ being given the same value in margarite, muscovite and paragonite.

For chloritoid the activity composition relations are updated from those in White *et al.* (2000). Recognizing that chloritoid is characterized by two types of layer in which Al and Fe^{3+} can only mix on one M1A site, its end-member formulae may be written as:

fctd: $Fe_2Al_3AlSi_2O_8(OH)_4$

mctd: $Mg_2Al_3AlSi_2O_8(OH)_4$

mnctd: $Mn_2Al_3AlSi_2O_8(OH)_4$

ctdo: $Fe_2Al_3Fe^{3+}Si_2O_8(OH)_4$

and activities are given by:

$$a_{\text{fctd}} = X^2_{\text{Fe M1B}} X_{\text{Al M1A}} \gamma_{\text{fctd}}$$

$$a_{\text{mctd}} = X^2_{\text{Mg M1B}} X_{\text{Al M1A}} \gamma_{\text{mctd}}$$

$$a_{\text{mnctd}} = X^2_{\text{Mn M1B}} X_{\text{Al M1A}} \gamma_{\text{mnctd}}$$

$$a_{\text{ctdo}} = X^2_{\text{Fe M1B}} X_{\text{Fe}^{3+}\text{M1A}} \gamma_{\text{ctdo}}$$

and all non-ideality taken as symmetric (regular solution) with $W_{\text{fctd mctd}} = W_{\text{fctd mnctd}} = W_{\text{mctd mnctd}} =$ 1.0 kJ and all Ws involving ctdo being set to zero. The Gibbs energy of end-member ctdo was made from $2G_{\text{fctd}} + (G_{\text{hem}} - G_{\text{cor}})/2 + 25.0$ kJ.

For carpholite the activity composition relations are updated from those in Coggon & Holland (2002), with its end-member formulae written as

fcar: $FeAlAl_2Si_2O_{10}(OH)_4$

mcar: $MgAlAl_2Si_2O_{10}(OH)_4$

mncar: $MnAlAl_2Si_2O_{10}(OH)_4$

caro: $FeFe^{3+}Al_2Si_2O_{10}(OH)_4$

and activities are given by:

$$a_{\text{fcar}} = X_{\text{Fe M1}} X_{\text{Al M2}} \gamma_{\text{fcar}}$$

$$a_{\text{mcar}} = X_{\text{Mg M1}} X_{\text{Al M2}} \gamma_{\text{mcar}}$$

$$a_{\text{mncar}} = X_{\text{Mn M1}} X_{\text{Al M2}} \gamma_{\text{mncar}}$$

$$a_{\text{caro}} = X_{\text{Fe M1}} X_{\text{Fe}^{3+}\text{M2}} \gamma_{\text{caro}}$$

and all non-ideality taken as symmetric (regular solution) with $W_{\text{fcar mcar}} = W_{\text{fcar mncar}} = W_{\text{mcar mncar}} =$ 1.0 kJ and all Ws involving caro being set to zero. The Gibbs energy of end-member caro was made from $G_{\text{fcar}} + (G_{\text{hem}} - G_{\text{cor}})/2 + 45.0$ kJ and mncar from $G_{\text{mcar}} + G_{\text{mang}} - G_{\text{per}} + 30.0$ kJ.

Activities for other phases are as follows: epidote (Holland & Powell, 1998), garnet (White *et al.*, 2005), chlorite (Holland *et al.*, 1998), staurolite (Mahar *et al.*, 1997) and carpholite.

Received 30 November 2009; revision accepted 27 April 2010.